C.2 16-bus System Presentation

The 16-bus system is a realistic test case used to apply the proposed GFM methodology. This system was first used in [117] and originates from a real area of the french transmission system. As such, the topology, installation ratings, and lines data are provided by the French TSO, RTE. In the following, the system is described and the three scenarios under study are detailed.

C.2.1 Description

The one-line diagram of the 16-bus system is recalled in Fig. C.3. The system hosts nine loads, two HVDC links, and three RES: RES 9 and 15 are aggregated onshore solar and wind while RES 12 is an offshore wind farm. The system is split into two regions interfaced by a transformer: buses 0 to 7 are on the 400 kV side, while the buses 8 to 12 are on the 225 kV side.

The external grid is represented by a stiff voltage source at bus 0. The 0-4 line impedance is set for the desired electric distance between the system and the external grid.

Two reactive power compensation devices are present in the system to maintain the buses voltage at acceptable values (±7% of the nominal voltage). Both devices are passive, modeled as shunt inductors. The inductor at bus 2 is set to deliver 216 MVAr at 380 kV, therefore $L_2 = 2.128\ H$, while the inductor at bus 15 delivers 240 MVAr at 225 kV which sets $L_{15} = 0.671\ H$.

The HVDC links and the RES are represented by the same model of VSC. The ratings of each converter are shown in Table C.7.

Table C.7: 16-bus system: converter data

	S_{nom} MVA	P_{nom} MW	U_{nom} kV
HVDC1	1388	1330	400
HVDC7	1044	1000	400
RES9	67.2	64.4	225
RES12	470	450	225
RES15	20	19	225

The transformer linking the 400 kV and 225 kV levels is the aggregated and equivalent model of three parallel YYD transformers, which are represented by a single YY transformer with the characteristics below:

Table C.8: 16-bus system: transformer data

	R pu	X pu	n	S_{nom} MVA
7 - 8	0.0011	0.1278	1.05	1200

The lines linking the system buses are all modeled as pi-section lines. This choice is due to the data made available by RTE, despite the lines linking buses 12 and 15 being undersea cables. The pi-model of the undersea cable is accepted as a first approximation because only SSS studies are conducted on the system and the frequency range considered ($< 500\ Hz$) remains low. The length and RLC properties of each line are detailed in Table C.9.

Table C.9: 400 kV line data

Line		Length (km)	$R(\Omega/km)$	$L(\Omega/km)$	$C(\mu F/km)$
1	2	24.56	0.01547231	0.257329	4.438111
2	3	14.248	0.03017967	0.3060079	3.790006
		14.3	0.03006993	0.3041958	3.776224
2	4	36	0.02	0.263	4.388889
		36	0.02	0.263	4.388889
		36.44	0.02000549	0.2630077	4.390779
		36	0.02	0.263	4.388889
4	5	14	0.02	0.263	4.428571
4	6	14	0.02	0.263	4.428571
5	7	69.804	0.02100166	0.3049968	3.81067
6	7	69.974	0.0210078	0.3049704	3.801412
8	9	10.247	0.06050552	0.4001171	2.927686
		10.238	0.05958205	0.4004688	2.93026
8	11	36.873	0.05993545	0.4049033	2.874732
8	13	5.096	0.06004709	0.4032575	2.747253
9	10	9.045	0.04532891	0.2144831	5.475954
9	11	41.605	0.05960822	0.4016344	3.316909
10	15	7.498	0.060016	0.4027741	2.934116
12	15	39.116	0.03451273	0.1413744	65.62762
		39.116	0.03451273	0.1413744	65.62762
13	14	1.511	0.06022501	0.3977498	2.647254
13	15	9.702	0.05998763	0.3979592	2.886003

C.2.2 Base Scenario

Similarly to the 4-VSC system, the loadflow is chosen such as no active nor reactive power flows to the external grid at bus 0, thus allowing the 0-4 line impedance to vary without altering the system OP. For all scenarios and GFM placement variants, the 0-4 line impedance maintains the same value: $X_{04} = 100\ \Omega$, which guarantees an unstable starting point in all case studies.

For the base scenario, the active and reactive power generated and/or consumed at each bus, along the bus voltage are presented in Table C.10. For HVDC links and RES, the active and reactive power are positive if the PEIR are injecting the power to the AC grid. Inversely, for the loads, the reactive power is positive if the load is consuming the reactive power (inductive load).

In this base scenario, all loads are passive and are modeled by parallel RC or RL branches depending on their power consumption set in Table C.10. As shown in Table C.10, most loads are capacitive. Recalling that the loads are aggregated distribution networks or smaller areas

Table C.10: Base Scenario Operating Point

Bus	Device	P (MW)	Q (MVAr)	U (pu)
0	External source	0	0	1
1	HVDC 1	1325	-343	0.98
2	Shunt Inductor	0	239	0.99
3	Load 3	129	-25	0.99
4	Load 4	674	-334	1
5	Load 5	42	-36	1
7	HVDC 7	976	-162	1
	Load 7	1125	-151	1
9	RES 9	9	0	1.07
	Load 9	68	-74	1.07
10	Load 10	23	-2	1.07
11	Load 11	275	-98	1.07
12	RES 12	90	-147	1.06
14	Load 14	2.9	0.6	1.06
15	RES 15	2.74	0	1.06
	Load 15	52	-25	1.06
	Shunt Inductor	0	269	1.06

within the studied system, this capacitive behavior reflects a realistic summer day scenario when the consumption is low, and the decentralized generation is high, leading to a lightly loaded network which results into a capacitive behavior of the transmission lines and voltages higher than the nominal voltage.

C.2.3 Topology and OP Change

In this second scenario, the loads remain passive and all VSC remain in GFL control. Additionally, the system is made less meshed by opening three of the four lines linking buses 2-4, one of the two lines linking buses 8-9, 9-10 and 9-11. The load at bus 7 is discarded, and HVDC 7 power flow is inverted to model a power export at bus 7.

Furthermore, more renewable power is available by setting all RES active power output at 70% of their nominal power. Moreover, all RES contribute to voltage support by injecting/absorbing reactive power up to 30% of their rated power.

Finally, the load at bus 4 is readjusted to ensure null power flow to the infinite source at bus 0.

The details of the active, reactive power and buses voltage are presented in Table C.11.

C.2.4 Active Loads

In this scenario, the topology and the loadflow pattern of the base scenario detailed in Table C.10 are adopted. However, a selection of loads is assumed to be active. The selected loads converted from passive to active are loads 5, 7, 9, 10, 14 and 15.

The active loads are controlled using a different GFL scheme. The control structure is shown in Fig. C.4, where the outer loops are discarded and the current references are

Table C.11: Topology and OP change Scenario Operating Point

Bus	Device	P (MW)	Q (MVAr)	U (pu)
0	External source	0	0	1
1	HVDC 1	1325	-347	0.95
2	Shunt Inductor	0	220	0.96
3	Load 3	129	-25	0.99
4	Load 4	318	-238	1
5	Load 5	42	-36	1
7	HVDC 7	-800	0	1
9	RES 9	47	-20	1.06
	Load 9	68	-74	1.06
10	Load 10	23	-2	1.05
11	Load 11	275	-98	1.07
12	RES 12	328	-140	1.06
14	Load 14	2.9	0.6	1.05
15	RES 15	14	-6	1.05
	Load 15	52	-25	1.05
	Shunt Inductor	0	269	1.05

directly set based on the active and reactive power set points. Assuming a power-invariant Park transformation and that the PLL regulates $v_{g_q}^f$ to 0, it follows that:

$$\begin{cases} i_d^* = \dfrac{P^*}{v_{g_d}^f} \\ i_q^* = \dfrac{-Q^*}{v_{g_d}^f} \end{cases} \tag{C.1}$$

Furthermore, the tuning used for the active loads is shown in Table C.12, the inputs filtering and switching frequency are identical to those in Table 2.2. It is assumed that the aggregated loads display a degraded performance and do not result from a dedicated SSS design study. As such, the PLL is faster, the current control is tuned using pole placement, and the voltage feedforward is kept on both axes.

Table C.12: Active loads GFL parameters

Control	Parameter	Value
PLL	ω_n	500 rad/s
	ξ	1
Current control	ω_{cc}	366 rad/s
	ξ_{cc}	1

The active loads are modeled as VSCs, the nominal power is chosen such as their active power reference corresponds to 60% of their nominal power. The nominal apparent power is calculated such as:

$$S_{nom}^{activeload} = \sqrt{(P_{nom}^{activeload})^2 + (Q_{\max}^{activeload})^2} \tag{C.2}$$

where $Q_{\max}^{activeload} = 0.3\ P_{nom}^{activeload}$.

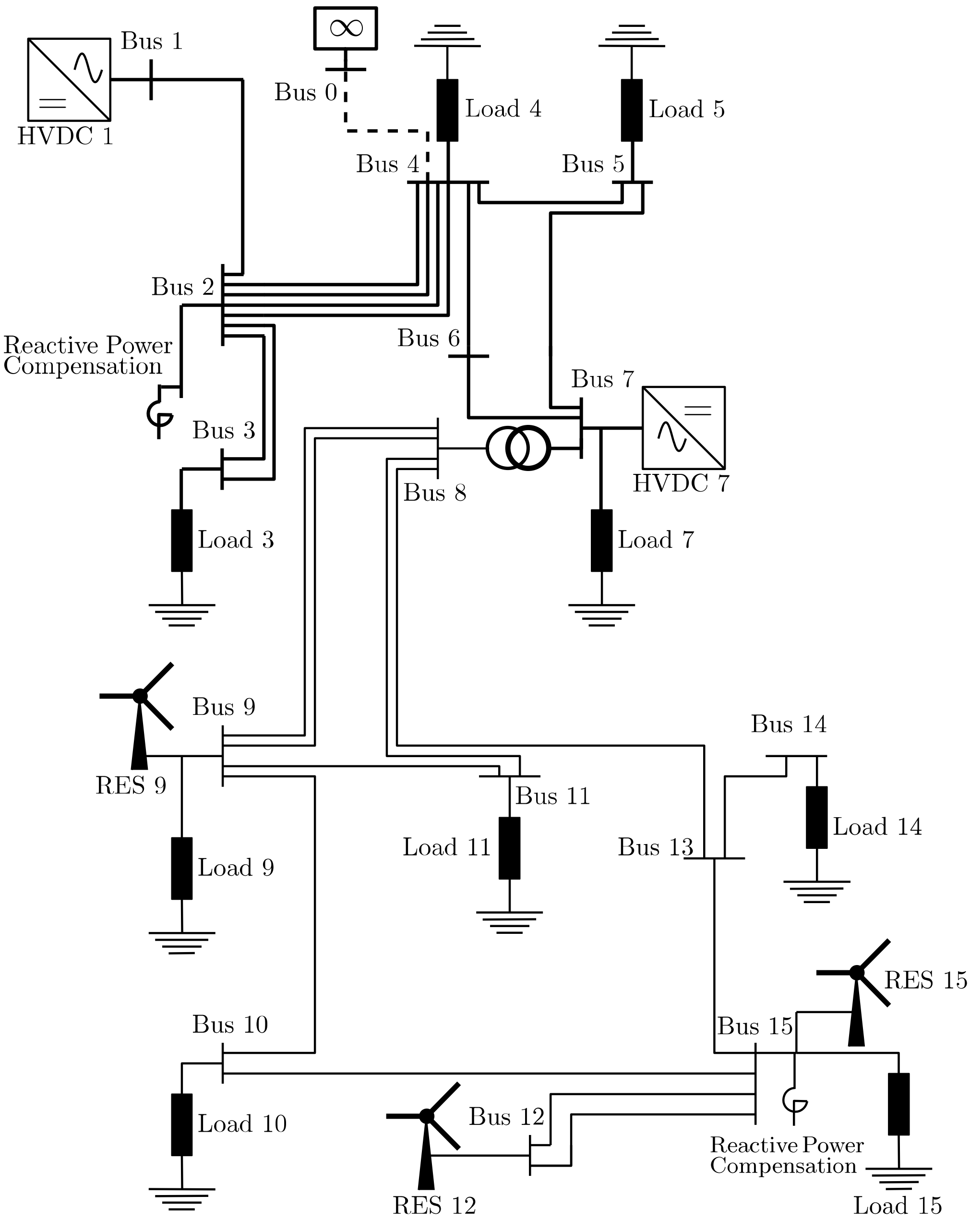

Figure C.3: Description of the 16-bus System

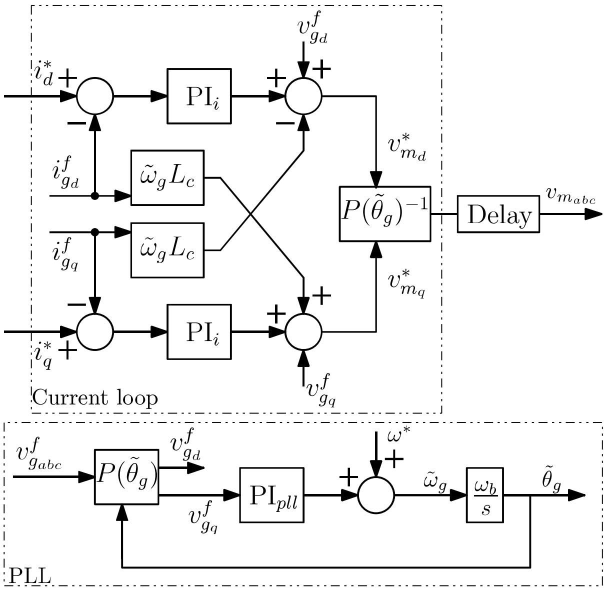

Figure C.4: Grid following Control Structure for Active Loads